A Study of Low Frequency Dielectric Dispersion of Lead-Free $0.94(Na_{0.50}Bi_{0.50})Ti_{0.95}V_{0.05}O_3$-$0.06BaTiO_3$ Ceramics

Anita Verma[1)], Arun Kumar Yadav[1)], Nasima Khatun[2)], Sunil Kumar[1)], Somaditya Sen[1,2,3,a)]

[1]Discipline of Metallurgy Engineering and Materials Science, Indian Institute of Technology Indore, Khandwa Road, Indore-453552, India
[2]Discipline of Physics, Indian Institute of Technology Indore, Khandwa Road, Indore-453552, India
[3]Dept. of Electrical Engg., Ming Chi University of Technology, New Taipei, Taiwan

a)Corresponding author: sens@iiti.ac.in

Abstract. A study of structure, morphology, and dielectric/complex impedance spectroscopy of lead-free $0.94(Na_{0.50}Bi_{0.50})Ti_{0.95}V_{0.05}O_3$-$0.06BaTiO_3$ ceramics, prepared by a modified sol-gel process, is explored. Rietveld refinement of x-ray diffraction confirmed the rhombohedral*R3c* phase. Temperature-dependent dielectric studies showed the antiferroelectric to paraelectric phase transition at a temperature, T_m~ 287 ºC.Complex impedance spectroscopy confirmed that the conductivity was found to increase from 1.8×10^{-8} $\Omega^{-1}cm^{-1}$ (for 240 ºC) to ~2.6×10^{-5} $\Omega^{-1}cm^{-1}$ (380 ºC) with increasing temperature.

INTRODUCTION

$PbZr_{0.52}Ti_{0.48}O_3$ (PZT), based materials are commercialized for actuators, sensors, electro-optic modulators, pyroelectric detectors, ultrasonic transducers, etc. applications. It has interesting piezoelectric and ferroelectric properties due to the existence of a morphotropic phase boundary (MPB)[1]. The major drawback of this compound, it contains about 60 wt. % of *Pb*, which is toxic and harmful for the environment. Due to the environmental concern European Commission, 2008 banned all lead-based materials for electronic applications. As a result, rising demands for the environment-friendly, lead-free materials such as $Na_{0.5}Bi_{0.5}TiO_3$ (NBT), $K_{0.5}Na_{0.5}NbO_3$ (KNN), $BaTiO_3$, and bismuth layered structure, etc[2-5] received more attention. Among all lead-free materials, NBT has gained notable attraction due to its high remnant polarization P_r~ 38 μC/cm^2, high depolarization temperature T_d ~ 200 °C and high Curie temperature ~ 320 °C[6]. Also, it has a large coercive field E_c~ 75 kV/cm and leakage current. These drawbacks restrict to pole the sample and use in the piezoelectric application. Large coercive field of this material is due to the volatile nature of Na and Bi at the high sintering temperature[7].

Many solid-solutions have been investigated, like $Na_{0.5}Bi_{0.5}TiO_3$-$BaTiO_3$ (NBT-BT), $Na_{0.5}Bi_{0.5}TiO_3$-$K_{0.5}Na_{0.5}NbO_3$, and $Na_{0.5}Bi_{0.5}TiO_3$-$SrTiO_3$ etc. [8, 9] Lead-free NBT-BT ceramics reveal a MPB at x ~ 0.06 composition (NBT-6BT), similar to PZT [10]. Unpoled NBT-6BT ceramics are in rhombohedral*R3c* " pseudo-cubic" like structure at room-temperature with anti-phase octahedral ($a^-a^-a^-$) tilt [9]. The motivation of present work is a study of structure, morphology, dielectric properties of $0.94(Na_{0.50}Bi_{0.50})Ti_{0.95}V_{0.05}O_3$-$0.06BaTiO_3$, [named as NBT6BT5V]ceramics prepared via a modified sol-gel method. Temperature-dependent, complex impedance spectroscopy was used to estimate the conductivity of NBT6BT5V sample.

EXPERIMENTAL

Polycrystalline NBT6BT5V powders were synthesized using the modified sol-gel method. For synthesis, sodium nitrate (purity 99.9%), bismuth nitrate (purity 99.9%), barium nitrate (purity 99.9%), dihydroxybis (ammonium lactate) titanium (IV), 50% w/w aqua solution (purity 99.9%), and vanadium oxide (purity 99.9%), all from Alfa Aesar, were chosen as precursors (Alfa Aesar). For each precursor, stoichiometric solutions were prepared in different beakers. All solutions were mixed in a big beaker (2 liters) and stirred for 2h at room

temperature. A mixture of ethylene glycol and citric acid 1:1 molar ration was vigorously stirred and heated (at ~85 °C on a hot plate) to form a gel. The cations get attached to the polymer chains of the gel which were later burnt in open air inside a fume hood. The burnt powders were ground carefully in a mortar and pestle. For decarburization and denitrification powder was heated at 500 °C for 12 h. After that, the resultant powders were heated at 700 °C for 10h for calcination. The powders were mixed with 5 weights % PVA (Polyvinyl alcohol) solution and pressed in a uniaxial hand press into discs of 10 mm diameter and 1.5 mm thickness. These pellets were sintered at 600°C for 6 h to evaporate the binder and further continued to be sintered at 1100 °C for 3 h to form mechanically dense pellets. Powder x-ray diffraction was performed using a Bruker D2 Phaser X-ray Diffractometer to confirm the phase purity and structure of the sample. The microstructures of sintered pellets were investigated by Supra55 Carl Zeiss Field Emission Scanning Electron Microscope (FESEM). Dielectric data were measured using a Newtons 4th LTD phase sensitive multimeter with signal strength of 1Vrms.

RESULTS AND DISCUSSION

To investigate the structural properties, Rietveld refinement was carried out on XRD data at room temperature using Fullprof software[11]. The XRD data was well fitted by rhombohedral*R*3*c* phase with acceptable R-factors (R_p, R_{wp}, and R_{exp}) [Fig. 1].

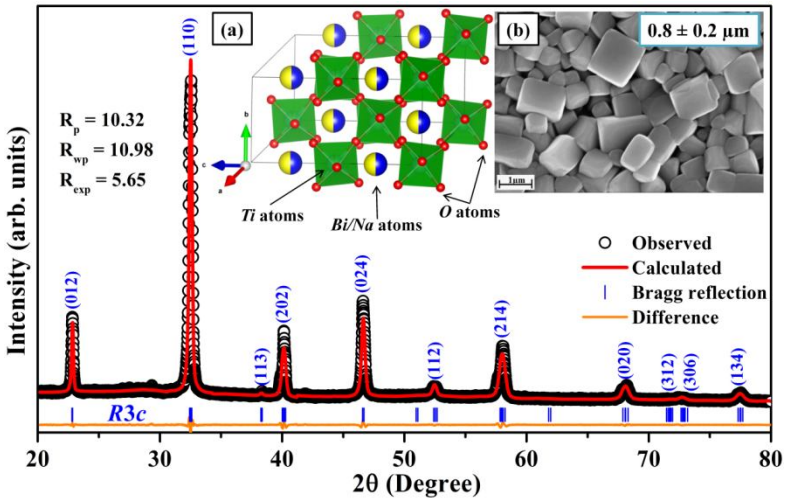

Figure 1. Rietveld fitted data by rhombohedral (with space group *R*3*c*) of NBT6BT5V, inset figures, where (a) Unit cell structure, projection from [*xyz*]direction, and (b) FESEM image of the sintered pellet at 1100 °C for 3h.

Bragg peaks were modeled using a Pseudo-Voigt axial divergence asymmetry function. A background was estimated by linear interpolation. Scale parameters, lattice parameters, half-width parameters, and position parameters of various lattice sites for all atoms were refined one by one. From, the final cycle of refinement, lattice parameters a = b= 5.4691(6) Å and c = 13.4653(14) Å, α = β = 90° and γ = 120° are obtained. The average unit cell volume is ~348.79 (23) Å^3, with a unit cell distortion (η %) ~ 0.5 estimated at room temperature. To visualize the unit cell structure of rhombohedral*R*3*c*, a geometrical structure is drawn using the refined CIF (crystallographic information file) file. A-site cations (Na/Bi/Ba) off-centering and anti-phase octahedral tilting ($a^-a^-a^-$) are shown from projection [*xyz*] direction [Inset Fig.1a]. Surface morphology of sintered pellet is shown in inset Fig.1b. A well dense morphology constituted of cuboid particles is observed. The relative density was calculated (Experimental density*100/Theoretical density) ~ 91% obtained for the sintered pellet at 1100 °C for 3 h. The average grain size was ~0.8 ± 0.2 µm estimated using the image J software.

A temperature-dependent (50-400 °C) dielectric measurement at some fixed frequencies was carried out to investigate the phase transformation behavior of NBT6BT5V sample. Two types of dielectric anomalies are observed; ferroelectric to antiferroelectric (FE→AFE) and antiferroelectric to paraelectric (AFE→PE) [Fig. 3a]. The diffused nature of this dielectric anomaly might arise from A/B-site lattice disorders[12, 13]. The anomaly around FE→AFE transition seems to be quite diffused, and hence the transition temperature is difficult to be estimated. The AFE→PE transition temperature (T_m) was estimated ~287 ºC. Low - frequency dispersion was observed in ε_r at T_m. These types of relaxations are related to migration and accumulation of electric charge carrier at the grain

boundaries in the externally applied field. This phenomenon is known as space charge polarization.If the applied ac field is reversed with the rate less than the space charge polarization, the dielectric dispersion can observed[14]. With an increase in applied ac field frequency, this effect is decreased. The ε_r is plotted as a function of frequency at different temperatures [Fig. 3b]. $\varepsilon_r$has higher values at low frequency,starts to an increase with increasing temperature. Most probably this is due to increase in space charge polarization with increasing temperature. With increasing frequency this effect is suppressed[15, 16].

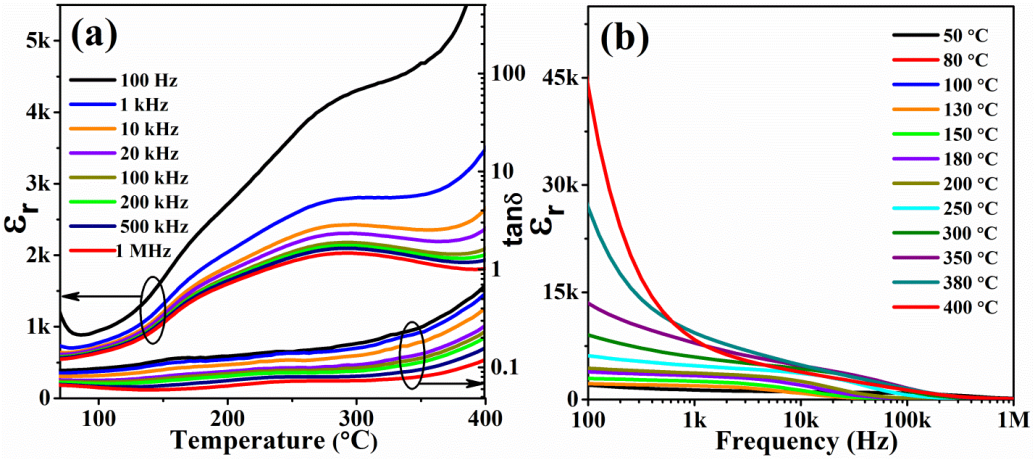

Figure 3. (a) Temperature dependent dielectric constant (ε_r) and loss tangent (tanδ) for NBT6BT5V sample at different frequencies, and (b) ε_r versus frequency at different temperatures.

To investigate the conduction mechanism in NBT6BT5V sample, complex impedance spectroscopy was performed at different temperatures from 1 Hz to 1 MHz range. AC complex impedance data of NBT6BT5V ceramic sample measured at different temperatures along with fitted Nyquist plots of these data at 240 ºC, 350 ºC, and 380 ºC are shown in Figs. 4(a-b). Generally, three semicircles are observed in Nyquist plot, the first smaller semicircle results from grain contribution (at higher frequency side), second one due to grain boundary (at lower frequency side), and third one due to electrode contribution. Out of these three semicircles, only single semicircle was observed for 240 ºC, 350 ºC, and 380 ºC temperature. Note that It seems that the sample has lesser resistance for grain boundaries and hence the second semicircle has merged with the first, i.e., the grain effect[16]. Resistance was estimated ~ 54.8 ΩM (at 240 ºC), ~ 23.9 ΩM (350 ºC), and ~ 39.2 kΩ, decreases with increasing temperature. Conductivity was calculated ~ 1.8×10^{-8} $\Omega^{-1}cm^{-1}$ (at 240 ºC), 4.2×10^{-8} $\Omega^{-1}cm^{-1}$ (350 ºC), and 2.6×10^{-5} $\Omega^{-1}cm^{-1}$ (380 ºC) increases with increasing temperature. Also, low-frequency tailing was observed at high temperature [Fig. 4b] which may be due to ion-blocking electrodes[17]. This is a characteristic feature of ionic conductors. At low temperatures, linear plots were observed due to the high resistance of the sample.

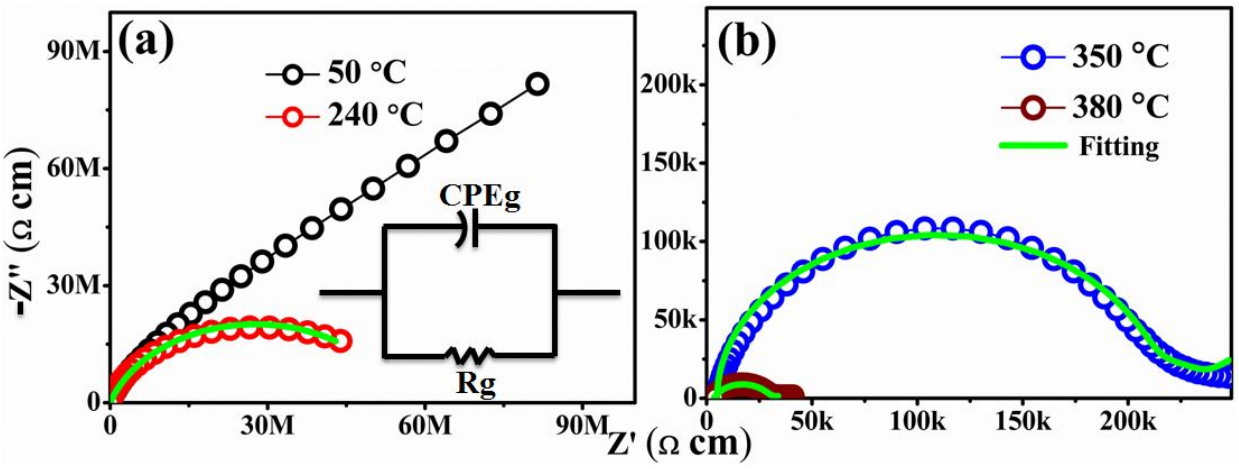

Figure 4. Nyquist plot (imaginary impedance ($-Z''$) versus real impedance (Z') curve) of NBT6BT5V sample at different temperatures, where (a) 50 ºC, 240 ºC (b) 350 ºC and 380 ºC. Inset Fig. a is showed the equivalent circuit diagram.

CONCLUSIONS

Lead-free NBT6BT5V ceramic powders were successfully synthesized using the modified sol-gel method. Rietveld refinement of XRD data confirmed the rhombohedral (with *R*3*c* space group) phase. FESEM image analysis reveals the dense morphology of cuboid particles with average grain size ~ 0.8 ± 0.2 μm. A temperature-dependent dielectric study showed the AFE→FE phase transition temperature, T_m ~ 287 ºC. Complex impedance revealed that conductivity was estimated ~ 1.8×10^{-8} $\Omega^{-1}cm^{-1}$ (at 240 ºC), 4.2×10^{-8} $\Omega^{-1}cm^{-1}$ (350 ºC), and 2.6×10^{-5} $\Omega^{-1}cm^{-1}$ (380 ºC), increases with increasing temperature. Low-frequency tail in Nyquist plot reveals the possibility of ionic conduction in this sample.

ACKNOWLEDGMENTS

Principle investigator expresses sincere thanks to the Indian Institute of Technology, Indore, India for funding the research. Authors would also like to thank Sophisticated Instrument Centre (SIC), IIT Indore for FESEM data.

REFERENCES

1. B. N. Rao, M. Avdeev, B. Kennedy and R. Ranjan, Phys. Rev. B **92** (21), 214107 (2015).
2. N. Zhao, H. Fan, L. Ning, J. Ma and Y. Zhou, J. Am. Ceram. Soc. **0** (0) (2018).
3. J. Wu, D. Xiao and J. Zhu, Chem. Rev. **115** (7), 2559-2595 (2015).
4. C. Reis, A. C. Silva, R. Guo, A. S. Bhalla and J. D. S. Guerra, presented at the 2014 Joint IEEE International Symposium on the Applications of Ferroelectric, International Workshop on Acoustic Transduction Materials and Devices & Workshop on Piezoresponse Force Microscopy, 2014 (unpublished).
5. A. Verma, A. K. Yadav, S. Kumar and S. Sen, AIP Conf. Proc. **1942** (1), 030024 (2018).
6. H. Yuji, W. Tomomi, N. Hajime and T. Tadashi, Jpn. J. Appl. Phys. **47** (9S), 7659 (2008).
7. E.-M. Anton, W. Jo, D. Damjanovic and J. Rödel, J. Appl. Phys. **110** (9), 094108 (2011).
8. S. Swain, P. Kumar, D. K. Agrawal and Sonia, Ceram. Int.**39** (3), 3205-3210 (2013).
9. R. Ranjan and A. Dviwedi, Solid State Commun. **135** (6), 394-399 (2005).
10. W. Jo, S. Schaab, E. Sapper, L. A. Schmitt, H.-J. Kleebe, A. J. Bell and J. Rödel, J. Appl. Phys. **110** (7), 074106 (2011).
11. H. Rietveld, J. Appl. Crystallogr. **2** (2), 65-71 (1969).
12. A. K. Yadav, A. Verma, S. Kumar, V. Srihari, A. K. Sinha, V. R. Reddy, S. W. Liu, S. Biring and S. Sen, J. Appl. Phys. **123** (12), 124102 (2018).
13. A. Verma, A. K. Yadav, N. Khatun, S. Kumar, R. Jangir, V. Srihari, V. R. Reddy, S. W. Liu, S. Biring and S. Sen, Ceram. Int. (2018).
14. J. Suchanicz, Mater. Sci. Eng., B**55** (1), 114-118 (1998).
15. B. K. Barick, K. K. Mishra, A. K. Arora, R. N. P. Choudhary and K. P. Dillip, Journal of Physics D: Applied Physics **44** (35), 355402 (2011).
16. A. K. Yadav, Anita, S. Kumar, A. Panchwanee, V. R. Reddy, P. M. Shirage, S. Biring and S. Sen, RSC Adv. **7** (63), 39434-39442 (2017).
17. T. Pareek, B. Singh, S. Dwivedi, A. K. Yadav, Anita, S. Sen, P. Kumar and S. Kumar, Electrochim. Acta **263**, 533-543 (2018).